This chapter was originally published in the book *Advances in Quantum Chemistry, Vol. 76* published by Elsevier, and the attached copy is provided by Elsevier for the author's benefit and for the benefit of the author's institution, for non-commercial research and educational use including without limitation use in instruction at your institution, sending it to specific colleagues who know you, and providing a copy to your institution's administrator.

CHAPTER SIX

Local Effective Hartree–Fock Potentials Obtained by the Depurated Inversion Method

Alejandra M.P. Mendez, Dario M. Mitnik[1], Jorge E. Miraglia
Instituto de Astronomía y Física del Espacio (IAFE), CONICET-Universidad de Buenos Aires, Buenos Aires, Argentina
[1]Corresponding author: e-mail address: dmitnik@df.uba.ar

Contents

Abstract

In this work we show the results of a numerical experiment performed on the Hartree–Fock (HF) wave functions in order to understand the relationship between the positions of the orbital nodes and the inflection points (zeros of their second derivative). This analysis is equivalent to investigating the existence of a physical one-electron local potential representing the interactions between the electrons. We found that with successive improvements in the quality of the numerical methods, the nodes and the inflection points systematically become closer. When the nodes coincide exactly with the inflection points, the existence of an effective local potential would be proven. However, this requirement cannot be fulfilled unless an explicit constraint (missing in the standard method) is incorporated into the HF procedure. The depurated inversion method (DIM) was devised to obtain detailed nl-orbital potentials for atoms and molecules. The method is based on the inversion of Kohn–Sham-type equations, followed by a further careful optimization which eliminates singularities and also ensures the fulfillment of the appropriate boundary conditions. The orbitals resulting from these potentials have their internal inflection points located exactly at the nodes. In this way, the DIM can be employed to obtain effective potentials that accurately reproduce the HF orbitals.

117

1. INTRODUCTION

The Hartree–Fock (HF) method is one of the best known and most commonly used approximation procedures to solve atomic, molecular, and solid systems because it greatly simplifies the problem of many electrons moving in a potential field. The method assumes, in accordance with the independent particle approximation and the Pauli exclusion principle, that the exact many-body wave function has the form of an antisymmetrized product of one-electron orbitals. After a self-consistent variational approach has been applied, a set of coupled equations for the orbitals is derived. Besides the minimization of the energies, the orbitals defining the wave function of the system are required to be orthonormal to each other. No further restrictions are imposed on the solutions.

In the present work, we will focus on the nodes of the HF orbitals and the radial location of their inflection points (the zeros of their second derivative). We will examine whether the orbital nodes can also be inflection points. Our investigation is based on a numerical experiment that studies in detail the influence of the methods employed for solving the HF equations on the radial location of the nodes and inflection points of the orbitals. The relative positions of these zeros are very important, since if they were not exactly at the same place, it would be impossible to obtain, through inversion, physical effective local potentials representing the interaction between the electrons. Based on our findings, we are tempted to postulate that although it is not explicitly required in any HF procedure, the nodes of the orbitals must also be turning points.

In a previous study,[1] a depuration inversion method (DIM) was devised. The method is based on the inversion of one-electron Kohn–Sham (KS) equations, whose solutions have been replaced by HF orbitals and energies. A further optimization procedure allows well-behaved effective potentials to ensue which, in turn, reproduce the original HF solutions very accurately. However, the new solutions have the advantage of having their internal inflection points located exactly at the same place as their nodes. Thus, our method can be considered as a means to introduce this additional constraint into the HF orbitals.

The chapter is organized as follows. In Section 2.1 the relative radial positions of the nodes and inflection points of the HF orbitals and their relationship with the accuracy of the computational calculations are analyzed. The origin of unphysical singularities in the effective potentials, due to

the inversion procedure, is described in Section 2.2. The characteristics of these features are also analyzed in terms of the accuracy of the numerical calculations. In Section 2.3 the DIM method, conceived for handling the numerical problems encountered in the inversion procedure, is briefly formulated. Section 3 shows an example of how we are able to obtain local effective potentials that accurately replicate the HF wave functions by applying the DIM method. Atomic units are assumed throughout, unless stated otherwise.

2. THEORY

2.1 HF Nodes and Derivatives

In this section we study the nodes of HF orbitals and their inflection points. The analysis is supported by using an example (the 2s orbital of the magnesium atom), however, the conclusions are valid for all the atoms, for any level. The orbital u_{2s}^{HF} and its second derivative $u_{2s}^{HF''}$ (multiplied by 0.1) are shown in Fig. 1 with solid and dashed lines, respectively. The orbital has one node and two inflection points. One of them, the external, is placed at $r \approx 0.9$ a.u. corresponding to the classical turning point. Beyond that point, the orbital decreases exponentially. The internal inflection point ($r \approx 0.18$ a.u.) is located, at first glance, at the same radius as the orbital node.
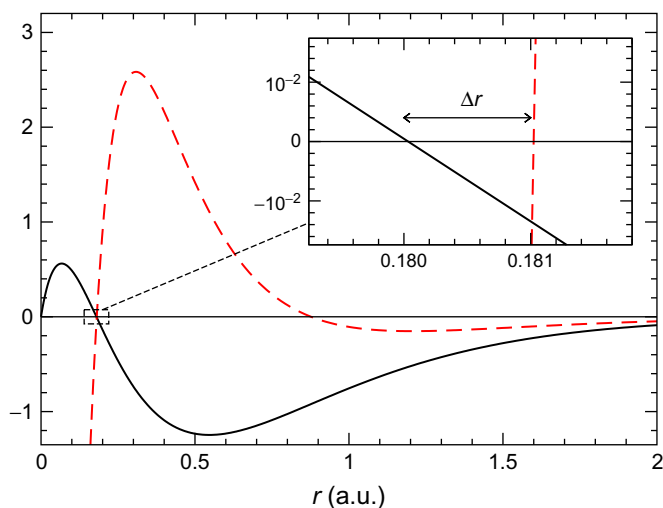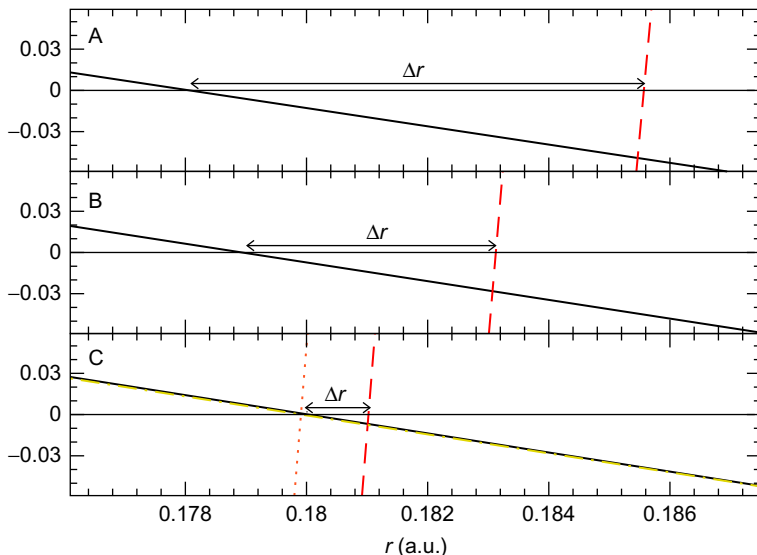

Fig. 1 Hartree–Fock orbital u_{2s}^{HF} (*solid line*) and scaled (×0.1) second derivative $u_{2s}^{HF''}$ (*dashed line*) corresponding to the ground state of magnesium atom.

A question arises concerning the coincidence of the location of these points: is this the consequence of a restrictive condition of the HF method or is it just a fortuitous outcome? The later possibility is discarded since the same results are found systematically in all the orbitals of any atom. However, if this is a strict requirement, one should expect an explicit constraint in the HF procedure, forcing that. Moreover, a more meticulous inspection of the calculated orbital (see inset of Fig. 1) shows that the inflection point (dashed line) is not located exactly at the node position. Defining Δr as the distance between the node of the orbital $u_{nl}^{\mathrm{HF}}(r)$ and the closest zero of the corresponding second derivative $u_{nl}^{\mathrm{HF}''}(r)$, there is a distance of $\Delta r = 10^{-3}$ a.u. between these zeros in the $2s$ orbital example. We found about the same Δr in many other cases. Of course this distance can be considered negligible but there is no constraint within the HF procedure, imposing the exact coincidence of both positions.

In spite of that, one could expect that both zeros (orbital and second derivative) must coincide exactly, i.e., the nodes must also be internal inflection points. More precisely, one may be inclined to think that Δr should be exactly zero. If this hypothesis is proven to be true, it could be added as a constraint when performing HF calculations. The numerical experiment designed to scrutinize this hypothesis consists in performing variousapproximations with successive improvements of their accuracy, examining the behavior of the corresponding Δr. The quality of the numerical methods for solving the HF equations can be evaluated through the variation of the numerical algorithm accuracy order and by changing the density of points of the numerical grids. In the present work we used the linear multistep Adams–Moulton method for the differential equations and the Lagrangian differentiation method for the derivatives. The methodology proposed is implemented by modifying the NRHF code by Johnson (see Ref. 2 for further details), which uses eighth-order approximations as default. Nevertheless, the same results and conclusions were obtained with other codes, for example, the HF code by Fischer.[3]

Fig. 2 shows the HF orbitals u_{2s}^{HF} (solid lines) and their second derivative $u_{2s}^{\mathrm{HF}''}$ (dashed lines) in the proximity of the node. The least accurate calculation, in which all numerical methods are taken at their first order, is shown in Fig. 2A. In this calculation we used a numerical grid with 200 points—the minimum number needed to achieve convergence. This gave the biggest value for $\Delta r = 8 \times 10^{-3}$. Increasing the grid density to 400 points, this distance decreases significantly, $\Delta r = 4 \times 10^{-3}$, as shown in Fig. 2B. The best

Fig. 2 Hartree–Fock orbital u_{2s}^{HF} and $u_{2s}^{HF''}$ (*solid* and *dashed lines*) when using (A) 200, (B) 400 points grid, and first-order approximations; (C) 1000 points grid and eighth-order approximation, u_{2s}^{OEP} and $u_{2s}^{OEP''}$ (*dot-dashed* and *dotted line*).

calculation performed is shown in Fig. 2C. In this case, an eighth–order approximation was considered in all the computational methods and a numerical grid of 1000 points was used. This arrangement led to the smallest difference $\Delta r = 1 \times 10^{-3}$. We were unable to obtain further improvements by increasing the number of points.

We performed an additional calculation using the optimized effective potential (OEP) method,[4,5] developed by Talman.[6] Fig. 2C also depicts the orbital u_{2s}^{OEP} near the node with dot–dashed line. However, because of the local character of the potential, its second derivative $u_{2s}^{OEP''}$—dotted line—is zero at the node.

We have recently developed the DIM[1] that enables one to acquire effective potentials which, in turn, reproduce the HF wave functions and energies very accurately. As we will see in the following section, the DIM potentials are physical, i.e., they have no singularities and they have the appropriate boundary conditions. The resulting orbitals have nodes that are also inflection points, a characteristic missing from the original HF orbitals. Unlike the OEP, the DIM effective potentials are orbital specific. This allows to obtain orbital inner shells energies much more accurately.

2.2 Inverted Effective Potentials

There are several methods to obtain effective potentials that describe a many-electron system. In principle, there is a direct way of calculating such potentials when the wave function is known, by inversion of the corresponding Schrödinger equations. The inversion scheme has been applied in different frameworks, from the density functional theory[7–9] to exact soluble models.[10] The procedure has been also applied in the calculation of atomic polarizability[11,12] and photoionization processes of atoms[13,14] and molecules.[15–17]

In our methodology,[1] we assume that the HF is turned into a set of KS–type equations, whose solutions are the HF orbitals and energies:

$$\left[-\frac{1}{2}\frac{d^2}{dr^2} + \frac{l(l+1)}{2r^2} + V_{nl}^{\mathrm{HF}}(r) \right] u_{nl}^{\mathrm{HF}}(r) = \varepsilon_{nl}^{\mathrm{HF}}\, u_{nl}^{\mathrm{HF}}(r) . \tag{1}$$

The direct inversion of Eq. (1) leads to effective nl-specific inverted potentials,

$$V_{nl}^{\mathrm{HF}}(r) = -\frac{1}{2}\frac{u_{nl}^{\mathrm{HF}''}(r)}{u_{nl}^{\mathrm{HF}}(r)} + \frac{l(l+1)}{2r^2} - \varepsilon_{nl}^{\mathrm{HF}} . \tag{2}$$

The direct computation of this equation is known to pose serious numerical problems.[18] The presence of genuine nodes in the orbitals can lead to the existence of poles and unphysical features around them. From Eq. (2) it is clear that the requirement of $\Delta r = 0$ is an unavoidable imposition in order to allow the existence of an effective potential free of singularities. An additional difficulty arises at large radii. If the exponential decay of the orbitals is not rigorously reproduced by the second derivatives, the effective inverted potentials may diverge.

Both problems are illustrated in Fig. 3. In this figure we show the effective potential $V_{2s}^{\mathrm{HF}}(r)$ corresponding to the 2s orbital of Mg (in dashed line). The figure shows that the inverted potential exhibits a singularity at $r \approx 0.18$ a.u., which corresponds to the genuine node of u_{2s}^{HF}. As discussed above, the radial position of the inflection point is not located exactly at the node of the orbital (they are separated by Δr). This distance remains nonzero, even within a calculation at the highest order of accuracy, preventing complete cancellation of the node in the denominator of Eq. (2), and is responsible for the unphysical pole. The other unphysical divergence of the potential at $r > 3$ a.u. (inset) is a consequence of the asymptotic exponential decay of the orbital, unbalanced by its second derivative.
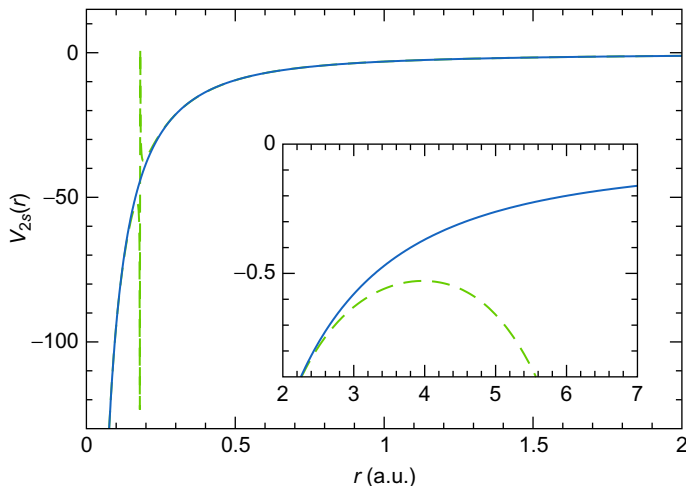
Fig. 3 Inverted V_{2s}^{HF} (*dashed line*) and depurated inverted V_{2s}^{DIM} (*solid line*) potential of the 2s orbital of magnesium atom.

A physical effective potential will allow generation of the corresponding structure of the system in a simple way. For example, for scattering process calculations it is convenient that the bound and continuum states should be computed on an equal footing. Nonetheless, requiring the existence of such a physical effective potential is not merely a demand of the atomic collision community. This requirement would be equivalent to imposing a $\Delta r = 0$ constraint in the HF procedure.

In the following, we will repeat the analysis performed above, but now the accuracy of the numerical methods involved in the calculations will be related to the appearance of the singularities of the effective potentials. To avoid handling the natural divergence due to the nucleus at the origin, we defined an *effective inverted charge*,

$$Z_{nl}^{HF}(r) = -rV_{nl}^{HF}(r). \tag{3}$$

The effective charge around the node located at $r \approx 0.18$ a.u. is shown in Fig. 4. The least accurate calculation, using only first-order approximations and 200 points in the numerical grid (dotted line), produces a relatively wide pole (its width is about 0.3 a.u.). By increasing the accuracy of the numerical methods and the density of points in the grid to eighth order and 1000 points (dashed line), respectively, we are able to reduce this width by an order of magnitude. A pole-less physical potential would allow to obtain, by solving
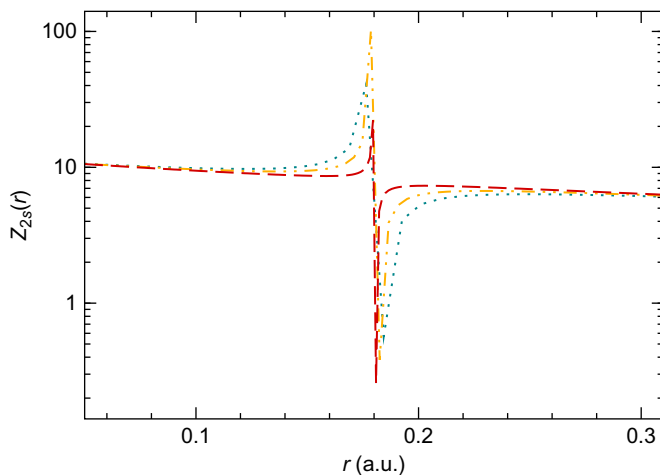
Fig. 4 Effective inverted charges around the node of u_{2s}^{HF} of Mg when different orders in the numerical method and grid densities are used.

the corresponding Schrödinger equation, orbitals having the internal inflection points at exactly the same location as its nodes.

The other feature of the potential considered above, related to its unphysical divergences at large distances (as a consequence of the different decreasing behavior between the wave functions and its second derivatives), can also be analyzed in terms of the accuracy of the numerical algorithms. In Fig. 5 we show the three calculations discussed previously. The least accurate calculation, corresponding to the first order in the numerical approximations (dotted line), shows a starting divergence at $r \approx 2$ a.u. Still, the best results for the effective inverted charge (dashed line) begin to diverge beyond 3 a.u.

We noticed an additional problematic feature in the HF solutions: the solutions may have oscillations (and therefore, spurious nodes) at the large r or "tail" region of the functions. These oscillations have already been pointed out by Fischer.[3] This failure to properly represent the orbitals is not caused by the numerical procedure but it is inherent to the method. Probably, due to the nonlocal character of the HF wave functions in which the behavior of a particular orbital depends on all others, these nodes may be attributed to surviving long-range exchange effects. Noticeably, we found the same spurious nodes at the same radial location even in calculations performed by using different numerical codes. As a general rule, the spurious nodes appear at very long distances, in regions where the amplitude of the orbital is very small. Therefore, their existence has no practical consequences and they can be effectively ignored in general.
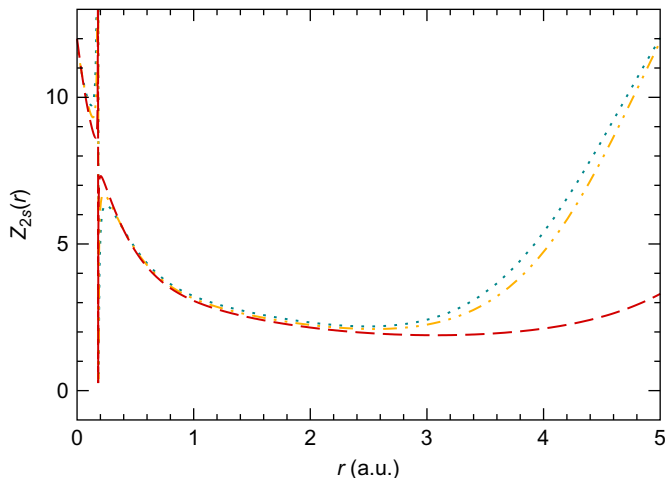
Fig. 5 Effective inverted charges computed with different orders in the numerical method and grid densities in the u_{2s}^{HF} of Mg atom.
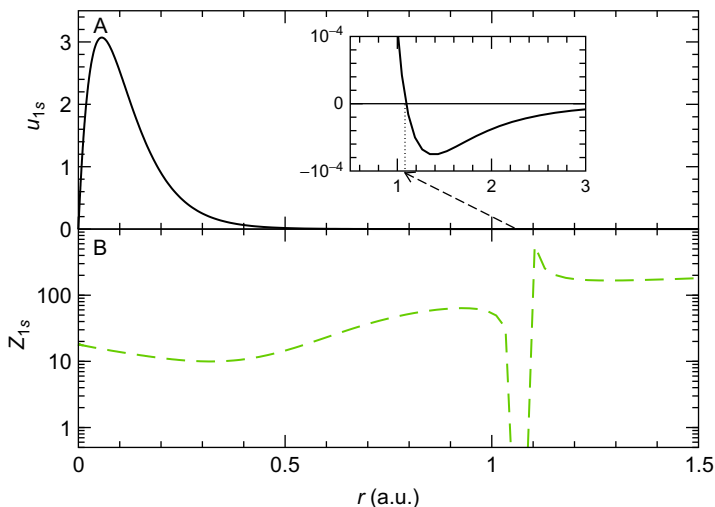
Fig. 6 (A) Hartree–Fock orbital u_{1s}^{HF} and (B) effective inverted charge Z_{1s}^{HF} of the 1s orbital of argon.

For example, the 1s orbital of the argon atom is nodeless, and it becomes practically zero for $r \geq 0.5$ a.u. However, a closer inspection shows a spurious node in the very large r region (at $r \approx 1.08$ a.u. as seen in Fig. 6A). Since the amplitude of the oscillation (see inset) is of the order of 10^{-4}, it passes generally unnoticed. Nonetheless, within the inversion scheme, the spurious node produces devastating effects. Evidence of this is the huge peak of

the effective charge $Z_{1s}^{HF}(r)$, as seen in Fig. 6B. As a matter of fact, the singularity is so big that it affects a broad range and causes the abrupt divergence of the effective charge for $r \geq 0.3$ a.u. This is really spectacular since a priori, there is no reason to suspect that a negligible oscillation in the tail of the wave function would produce such a big drawback at small distances. As a rule of thumb, we found that atoms with nuclear charge $Z_N \geq 13$ have spurious nodes, generally, in their most inner shells.

2.3 The Depuration Method

In order to deal with the problems of the inversion, we developed a complementary procedure. The depuration method consists, first, in erasing the unphysical poles and divergences from the inverted charges. Then, a parametric ad hoc formula is proposed in order to produce an analytic approximation to the charges. The physically correct boundary conditions are imposed through the proposed formula. The resulting effective potentials are then well behaved, without any singularity or divergence. A further optimization of the depurated potential is carried out. By solving iteratively the corresponding Schrödinger equation, orbitals u_{nl}^{DIM}, and energies ε_{nl}^{DIM} are obtained. Meanwhile, the fitting parameters are adjusted until the potential V_{nl}^{DIM} reproduces the original HF solutions with high accuracy.

We managed to constrain the potentials to have the right-boundary conditions by forcing the depurated inverted charge to behave as follows:

$$Z_{nl}^{DIM}(r) \equiv -rV_{nl}^{DIM}(r) \rightarrow \begin{cases} Z_N & \text{as } r \rightarrow 0 \\ 1 & \text{as } r \rightarrow \infty \end{cases} \tag{4}$$

where Z_N is the nuclear charge. Once the charge is determined at the boundaries, we can obtain a smooth analytic expression for $Z_{nl}^{DIM}(r)$ by fitting $Z_{nl}^{HF}(r)$ in the largest possible range, except at the regions where the charge has unphysical behavior (see Appendix for more details). This can be accomplished by enforcing the effective DIM charge to adjust the following analytical expression:

$$Z_{nl}^{DIM}(r) = \sum_j Z_j e^{-\alpha_j r} + 1 . \tag{5}$$

The asymptotic behavior defined by Eq. (4) is naturally fulfilled. In order to comply with the boundary condition at the origin, a further condition, $\Sigma Z_j = Z_N - 1$, is required for the fitting parameters.

The minimization of the adjustment parameters, Z_j and α_j, must be done carefully. Special attention should be paid to the adjustment region and the initial seeds chosen for the parameters. The fitting region is manually determined, that is, many points belonging to the original HF wave function should be discarded during the inversion procedure. Only the regions of the inverted charge with physical behavior must be preserved and considered, in such a way that Z_{nl}^{DIM} overlaps the inverted Z_{nl}^{HF} over a wide range. The unphysical behavior of the singularities and divergences are discarded. As the amplitude of the wave function becomes too small, the inversion must stop. Otherwise, the procedure diverges.

The most used optimization quantity in variational density functional approximation methods is the energy (some others consider the density). Although the minimization of the energy is a very important criterion, it is only one of the many observables that characterizes a quantum state. It has been proven that different functions (with different shapes) can produce, through a variational procedure, the same final energy. For instance Bartschat et al.[19,20] show a case in which two different potentials (one having exchange, the other neglecting it) led to very similar and accurate energies of the Rydberg series in several quasi–one-electron systems. However, a further examination of these potentials shows large discrepancies in scattering calculations.[21] Therefore, in addition to the energy, we have added the mean values of the orbitals as parameters in our variational procedure. This is achieved by optimizing the mean values $\langle 1/r \rangle$ (which characterize the quality of the wave function near the origin), and $\langle r \rangle$ (probing it at longer distances).

3. RESULTS

We denoted as u_{nl}^{DIM} and ε_{nl}^{DIM} the solutions obtained when the Schrödinger equation is solved with the depurated inverted potential V_{nl}^{DIM}.

In previous work,[1] the DIM was applied to ground state HF orbitals of several noble gases (He, Ne, Ar, and Kr) and the nitrogen atom. The potentials V_{nl}^{DIM} obtained reproduce wave functions and energies that agree with the HF ones with great accuracy. As a result of applying the depurated procedure, the singularities and divergences of the inverted potentials have been completely removed, and the V_{nl}^{DIM} potentials attained give a physically correct description of the problem.
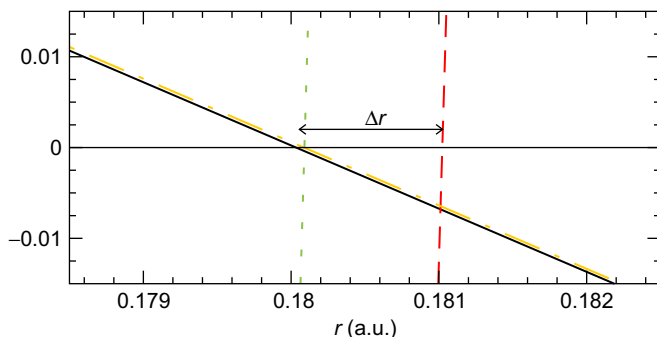
Fig. 7 Hartree–Fock orbital u^{HF} and corresponding second derivative $u^{HF''}$ (*solid and dashed lines*), DIM solved u^{DIM} and $u^{DIM''}$ (*dot-dashed and dotted lines*) for 2s orbital of magnesium.

Continuing with the example discussed in the previous section, a comparison between the DIM u_{2s}^{DIM} and the HF u_{2s}^{HF} orbitals of magnesium (and their corresponding second derivatives) is given in Fig. 7. The figure reproduces the inset of Fig. 1, additionally showing the DIM results (the corresponding V_{2s}^{DIM} potential is depicted in Fig. 3 with solid line). As stated above, the distance Δr, computed with eighth–order numerical approximations, between the nodes of u_{2s}^{HF}—dotted line—and the zero of its second derivative $u_{2s}^{HF''}$—dashed line—was found to be 1×10^{-3}. On the other hand, by using the V_{2s}^{DIM} potential, we obtained that the DIM second derivative $u_{2s}^{DIM''}$—dotted line—is zero exactly at the radius where the wave function u_{2s}^{DIM} —dash-dotted line—has a node.

As indicated previously, the conclusions reached here are general. They are valid for any other atom and for any level. We present the results for two additional atoms, boron and magnesium, in Table 1. The fitting parameters Z_j and α_j, defining the DIM charges (Eq. 5), allow to obtain orbital-specific potentials that, by solving the corresponding Schrödinger equation, replicate the original HF solutions within 1% and fulfill the $\Delta r = 0$ constraint.

4. CONCLUSIONS

The nodes and inflection points of the HF orbitals have been studied in detail. The influence of the quality of the numerical method used in the HF procedure was investigated. This was evaluated through the variation of the accuracy of the numerical algorithms and by changing the density of points in the numerical grids. The study showed that as the numerical quality

Table 1 Fitting Parameters for the Effective Charges of B and Mg Atoms for the Analytic Expression (5)

	nl	Z	α
B	1s	0.753400	6.14048
		1.43216	0.867257
		1.81444	0.905245
	2s	1.86154	1.10868
		0.153402	0.112430
		1.77713	2.40745
		0.207928	8.91487
	2p	1.69748	0.708184
		2.26098	3.54786
		0.041540	0.111029
Mg	1s	7.17402	1.31135
		3.38548	5.56370
		0.440500	1.26701
	2s	8.05058	3.30677
		2.74598	0.437365
		0.203440	22.3945
	2p	7.48607	2.78041
		1.28841	9.84139
		2.22552	0.475696
	3s	4.07701	6.01398
		6.18574	1.78888
		0.73725	0.665093

is improved, the distance Δr between the nodes of the HF orbitals and their inflection points became smaller. Further studies, considering higher orders in the numerical approximations, will allow one to perform an even more exhaustive inspection of these distances.

Therefore, one may propose the following hypothesis regarding these points: the nodes must be also inflection points. The similarities between

the OEP and the HF orbitals would suggest a way to endorse this premise. The conjecture may or may not prove to be true. Subsequent work should be done in order to settle this, one way or the other. If the conjecture is true, it could be added as a constraint when performing the HF calculations. This would also imply that there exists a local potential that generates the HF orbitals.

The DIM, briefly reviewed here, allows effective potentials to be obtained that, by solving the corresponding Schrödinger equation, generate orbitals and energies that agree with the HF solutions with great accuracy. The method consists in considering the direct inversion of KS-type equations with HF solutions, and a further optimization. The depuration method imposes physically correct boundary conditions and a specific analytical expression for the inverted potentials.

We asserted that there is a direct relationship correlating the distances between the nodes and the inflection points and the unphysical behavior of the inverted potentials. We concluded that by generating the physically DIM effective potentials, we are able to obtain (after its diagonalization) orbitals that comply the hypothesis and reproduce the HF solutions very accurately.

ACKNOWLEDGMENT

APPENDIX

The adjusting procedure consists in minimizing the function

$$\beta(x_i) = \gamma(x_i) - f(x_i, \lambda_1, \lambda_2, \ldots, \lambda_m), \tag{A.1}$$

which is the difference between the curve to be adjusted, $\gamma(r)$, and the adjusting function, $f(r)$. In the depurated inversion scheme, $\gamma(r) = Z_{nl}^{HF}(r)$ corresponds to the inverted charge, and $f(r) = Z_{nl}^{DIM}(r)$ corresponds to the analytical form we have set up for it (Eq. 5). In order to minimize $\beta(x_i)$ respect to the m parameters λ_j that determine f, we define the matrix elements A_{ij},

$$A_{ij} \equiv \frac{d\beta(x_i)}{d\lambda_j} = \frac{df(x_i, \lambda_1, \lambda_2, \ldots, \lambda_m)}{d\lambda_j} \tag{A.2}$$

Then, we obtain the system of equations

$$
\begin{bmatrix} d\beta(x_1) \\ d\beta(x_2) \\ \vdots \\ d\beta(x_n) \end{bmatrix} = \begin{bmatrix} A_{11} & A_{12} & \cdots & A_{1m} \\ A_{21} & A_{22} & \cdots & A_{2m} \\ \vdots & \vdots & \ddots & \vdots \\ A_{n1} & A_{n2} & \cdots & A_{nm} \end{bmatrix} \begin{bmatrix} d\lambda_1 \\ d\lambda_2 \\ \vdots \\ d\lambda_m \end{bmatrix}. \tag{A.3}
$$

By multiplying both sides of the equation with transpose matrix $[A]^T$,

$$
[A]^T[A][d\lambda] = [A]^T[d\beta], \tag{A.4}
$$

we are able to get a system of equations that can be solved with standard numerical routines. The solution $[d\lambda]$ allows one to obtain the best parameters that minimizes $[\beta]$.

REFERENCES

1. Mendez, A. M. P.; Mitnik, D. M.; Miraglia, J. E. Depurated Inversion Method for Orbital-Specific Exchange Potentials. *Int. J. Quantum Chem*. **2016**, *116*, 1882.
2. Johnson, W. R. *Atomic Structure Theory: Lectures on Atomic Physics*. Springer-Verlag: Berlin, Germany, 2007.
3. Froese Fischer, C.; Brage, T.; Jönsson, P. *Computational Atomic Structure: An MCHF Approach*. Institute of Physics Publishing: Bristol, UK, 1997.
4. Sharp, R. T.; Horton, G. K. A Variational Approach to the Unipotential Many-Electron Problem. *Phys. Rev.* **1953**, *90*, 317.
5. Talman, J. D.; Shadwick, W. F. Optimized Effective Atomic Central Potential. *Phys. Rev. A* **1976**, *14*, 36.
6. Talman, J. D. A Program to Compute Variationally Optimized Effective Atomic Potentials. *Comput. Phys. Commun*. **1989**, *54*, 85.
7. Wu, Q.; Yang, W. A Direct Optimization Method for Calculating Density Functionals and Exchange-Correlation Potentials From Electron Densities. *J. Chem. Phys*. **2003**, *118*, 2498.
8. Gaiduk, A. P.; Ryabinkin, I. G.; Staroverov, V. N. Removal of Basis-Set Artifacts in Kohn-Sham Potentials Recovered From Electron Densities. *J. Chem. Theory Comput.* 2013, *9*, 3959.
9. Ryabinkin, I. G.; Kohut, S. V.; Staroverov, V. N. Reduction of Electronic Wave Functions to Kohn-Sham Effective Potentials. *Phys. Rev. Lett*. **2015**, *115*, 083001.
10. Filippi, C.; Umrigar, C. J.; Taut, M. Comparison of Exact and Approximate Density Functionals for an Exactly Soluble Model. *J. Chem. Phys*. **1994**, *100*, 1290.
11. Sternheimer, R. M. Electronic Polarizabilities of Ions From the Hartree-Fock Wave Functions. *Phys. Rev.* **1954**, *96*, 951.
12. Dalgarno, A.; Parkinson, D. The Polarizabilities of Atoms From Boron to Neon. *Proc. R. Soc. Lond. A* **1959**, *250*, 422.
13. Hilton, P. R.; Nordholm, S.; Hush, N. S. The Ground State Inversion Potential Method: Application to the Calculation of Photoionization Cross Sections. *J. Chem. Phys.* **1977**, *67*, 5213.
14. Süzer, S.; Hilton, P. R.; Hush, N. S.; Nordholm, S. UV Subshell Photoionisation Cross-Section of Atomic Zn, Cd, and Hg: Experiment and Theory. *J. Electron Spectrosc. Relat. Phenom.* 1977, *12*, 357.

15. Hilton, P. R.; Nordholm, S.; Hush, N. S. Photoionization Cross Section of Water by an Atomic Extrapolation Method. *Chem. Phys. Lett.* **1979**, *64*, 515.

16. Hilton, P. R.; Nordholm, S.; Hush, N. S. Document Ground-State Inversion Method Applied to Calculation of Molecular Photoionization Cross-Sections by Atomic Extrapolation: Interference Effects at Low Energies. *J. Electron Spectrosc. Relat. Phenom.* **1980**, *18*, 101.

17. Crljen, Ž.; Wendin, G. Many-Body Theory of Effective Local Potentials for Electronic Excitations. III. Application to Giant Dipole Resonances. *Phys. Rev. A* **1987**, *35*, 1571.

18. Mura, M. E.; Knowles, P. J.; Reynolds, C. A. Accurate Numerical Determination of Kohn-Sham Potentials From Electronic Densities: I. Two-Electron Systems. *J. Chem. Phys.* **1997**, *106*, 9659.

19. Albright, B. J.; Bartschat, K.; Flicek, P. R. Core Potentials for Quasi-One-Electron Systems. *J. Phys. B* **1993**, *26*, 337.

20. Bartschat, K. *Computational Atomic Physics*. Springer-Verlag: New York, USA, 1996.

21. Bartschat, K.; Bray, I. Local Versus Non-Local Core Potentials in Electron Scattering From Sodium Atoms. *J. Phys. B* **1996**, *29*, 271.